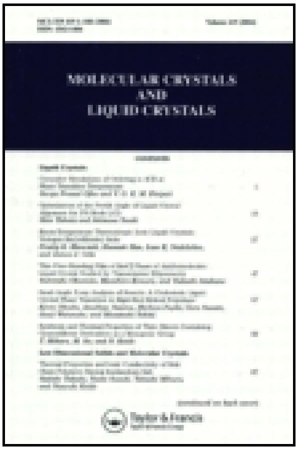

Molecular Crystals and Liquid Crystals Science and Technology. Section A. Molecular Crystals and Liquid Crystals

Publication details, including instructions for authors and subscription information:
http://www.tandfonline.com/loi/gmcl19

Expanding the Realm of Intercalation Chemistry: The Synthesis of Graphite and Metal Dichalco-genide Intercalates Containing Aromatic Hydrocarbons and Buckminster-fullerene, and the First Intercalates of Layered Metal Halides

Bruce A. Averill [a] , Thomas E. Sutto [a] & Jean-Marc Fabre [b]

[a] Dept. of Chemistry, University of Virginia, Charlottesville, VA, 22901, U.S.A.

[b] Laboratoire de Chimie Organique Structurale, Université de Montpellier II, 34095, Montpellier Cedex 5, France

To cite this article: Bruce A. Averill , Thomas E. Sutto & Jean-Marc Fabre (1994): Expanding the Realm of Intercalation Chemistry: The Synthesis of Graphite and Metal Dichalco-genide Intercalates Containing Aromatic Hydrocarbons and Buckminster-fullerene, and the First Intercalates of Layered Metal Halides, Molecular Crystals and Liquid Crystals Science and Technology. Section A. Molecular Crystals and Liquid Crystals, 244:1, 77-88

To link to this article: http://dx.doi.org/10.1080/10587259408050086

Mol. Cryst. Liq. Cryst. 1994, Vol. 244, pp. 77–88
Reprints available directly from the publisher
Photocopying permitted by license only

Printed in the United States of America

EXPANDING THE REALM OF INTERCALATION CHEMISTRY: THE SYNTHESIS OF GRAPHITE AND METAL DICHALCOGENIDE INTERCALATES CONTAINING AROMATIC HYDROCARBONS AND BUCKMINSTERFULLERENE, AND THE FIRST INTERCALATES OF LAYERED METAL HALIDES

BRUCE A. AVERILL and THOMAS E. SUTTO
Dept. of Chemistry, University of Virginia, Charlottesville, VA 22901 U.S.A.
JEAN-MARC FABRE
Laboratoire de Chimie Organique Structurale, Université de Montpellier II, 34095 Montpellier Cedex 5, France

Abstract Methods have been developed for the synthesis of novel intercalates of graphite, metal dichalcogenides (MY_2: M = Ti, Ta; Y = S, Se; M = Nb; Y = Se, Te) and metal halides $CuCl_2$; MBr_2: M = Ni, Cu, Cd; CdI_2). Aromatic hydrocarbons (pentacene (PEN), tetracene (TET), anthracene (ANT), 9,10-dichloroanthracene (DCA), and 9,10-dibromoanthracene (DBA)) have been intercalated into graphite, and PEN, TET, ANT have been intercalated into the metal dichalcogenides. Dibenzotetrathiafulvalene has been intercalated into MY_2 (M = Ti, Ta; Y = S, Se). In addition, C_{60} intercalates of TaS_2 and graphite have been prepared. Tetracyanotetrathiafulvalene was intercalated into 5 metal dihalides, forming the first known intercalates of these materials. The intercalates were structurally analyzed by X-ray powder diffraction, and the compositions determined experimentally. For all intercalates, the observed stoichiometries were in good agreement with those predicted from the X-ray data. The results of resistivity and magnetic susceptibility measurements on the intercalates are summarized.

INTRODUCTION

Three distinct types of layered compounds are known, which differ primarily in the charge on the layers and the types of interlayer forces responsible for holding the material together. The first contains neutral layers held together by van der Waals forces; examples include graphite, talc and the transition metal dichalcogenides (MY_2), phosphorus trisulfides (MPY_3), oxyhalides (MOX), and some dihalides (MX_2). The second consists of charged layers with ions of opposite charge holding the layers together by electrostatic (ionic) interactions; examples include the layered silicates and double hydroxides. The third type contains neutral layers that possess terminal hydroxyl groups that use hydrogen bonding to maintain the layered structure; examples include α-$Zr(HPO_4)_2{\cdot}H_2O$, γ-FeO(OH), and $Al(OH)_3$.

One of the most common reactions of such materials is the intercalation of various guest species between the host layers.[1] In virtually all cases examined to date, intercalation results in the formation of a new layered material in which the host layers acquire a net charge, which is compensated by the presence of oppositely charged guests (or species derived therefrom) within the galleries of the layered host. This type of intercalation reaction can occur: (i) via a redox reaction with hosts possessing neutral layers (to give species such as $TaS_2^-[Co(C_5H_5)_2]^+_{0.25}$ or $K^+C_8^-$); (ii) via an ion-exchange mechanism with hosts possessing charged layers (to give species such as Na^+ montmorillonite) or with neutral hosts (to give, e.g., $Mn_{0.8}PS_3K_{0.4}(H_2O)_{0.9}$); or (iii) via an acid-base reaction (e.g., formation of α-$[Zr(PO_4)_2](RNH_3^+)_2$).

In contrast, there are very few well-characterized examples of intercalation reactions of neutral hosts with no net redox or ion exchange reaction, in which the product is best formulated as containing neutral guest molecules inserted between uncharged guest layers.[2] Many apparent examples of neutral intercalates have been reported in the literature, such as the well-studied dichalcogenide-amine intercalates (e.g., $TaS_2 \cdot C_{18}H_{37}NH_2$). Recent detailed studies on the corresponding ammonia and pyridine intercalates, however, have shown that in most cases their formation proceeds via a redox reaction, with oxidation of NH_3 (to N_2 and NH_4^+)[2] and pyridine (to 4,4'-bipyridine and pyridinium)[3] and concomitant reduction of the host layers. These results suggest that the intercalation of amines and amides may also occur via analogous redox reactions, and indicate that more careful studies are needed.

The present work describes the synthesis, structures, and some properties of a number of novel intercalates of graphite, the metal dichalcogenides, and metal dihalides. In most cases the guests (Figure 1) are simple organic molecules with relatively high ionization potentials and low electron affinities, suggesting that non-specific (van der Waals) host-guest interactions are important factors in the formation of these compounds.

GENERAL PROCEDURE FOR PREPARATION OF INTERCALATES

The host material (ca. 0.2 g) is suspended in ca. 10 ml of an appropriate solvent (MeCN for graphite and MY_2, dry xylenes for MX_2) in a 5 dram (ca. 20 ml) sample vial and sonicated at full power for one minute using a Heat Systems - Ultrasonics, Inc. Model W-380 sonicator tuned to the frequency of the solvent (defined operationally as the frequency that gave the maximum amount of cavitation at full power.) Then 3 eq. of guest (1.0 g/0.2 g of graphite) was added, and the

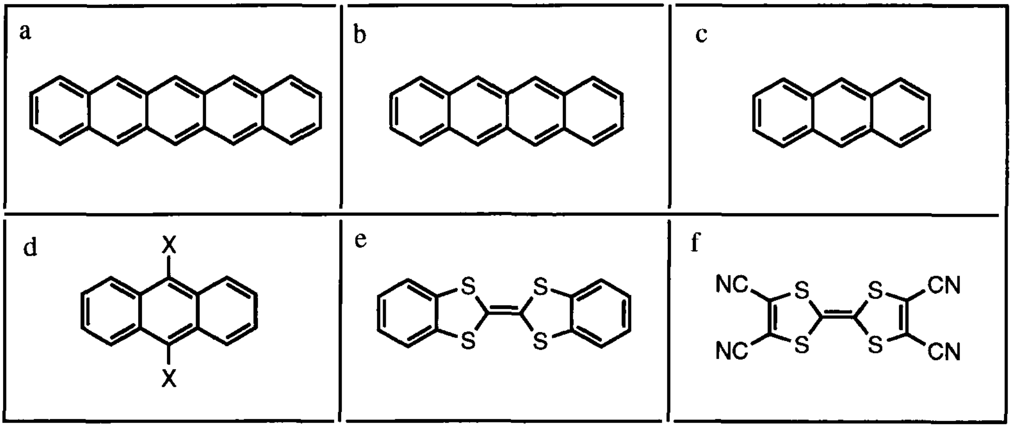

FIGURE 1. Schematic drawing of the structures of the organic guest molecules used in this research: (a) pentacene (PEN); (b) tetracene (TET); (c) anthracene (ANT); (d) X = Cl, 9,10-dichloroanthracene (DCA); X = Br, 9,10-dibromoanthracene; (e) dibenzotetrathiafulvalene (DBTTF); (f) tetracyanotetrathiafulvalene (TCN-TTF).

resulting suspension was sonicated again for 1 minute under the same conditions. The samples were then transferred to reaction flasks, flushed with argon, sealed, and heated at 60°C for one week. The samples were then filtered, washed with benzene, and dried *in vacuo* for 2 hours.

For intercalation of C_{60} into TaS_2 or graphite, the above method was ineffectual, and a more complex double displacement procedure was necessary. Thus, the n-octylamine (OA) intercalate of TaS_2, $TaS_2 \cdot (OA)_{0.39}$ was treated as above with a solution of C_{60}/C_{70} (ca. 90:10) in xylenes. Graphite·$FeCl_3$ (0.15 g) was added to ca. 125 ml of distilled 0.1 M HCl in H_2O, the resulting suspension was sonicated for 1 minute at full power, a solution of 400 mg C_{60}/C_{70} in 150 ml toluene was added, and the resulting heterogeneous mixture was sonicated at one-half power for 2 minutes and allowed to stand for 2 hours. The mixture was then filtered, and the solid was washed with benzene and dried *in vacuo*.

X-ray powder diffraction data were obtained on a Scintag powder diffractometer with a scan rate of 2°/min over a 2θ range of 5-75° in 0.01° steps and indexed using a Fortran IV X-ray fitting program.[4] Resistivity data were measured on a four-probe resistivity system using a Lake Shore temperature sensor with a calibrated Si diode (± 0.05 K) and a 20-mA (± 0.02 mA) constant current source. Resulting voltages were measured with a Keithley voltmeter with a sensitivity of 0.5 μV. Susceptibility data were obtained on a S.H.E. magnetic susceptometer operating at 25 kG for bulk magnetic susceptibility from 50 to 300 K. Compositions of the compounds were determined by elemental analysis and/or weight loss *in vacuo* at 100°C.

GRAPHITE INTERCALATES

The X-ray powder diffraction data observed for the new graphite intercalates are indicated diagrammatically in Figure 2, and relevant physical data are summarized in Table I.

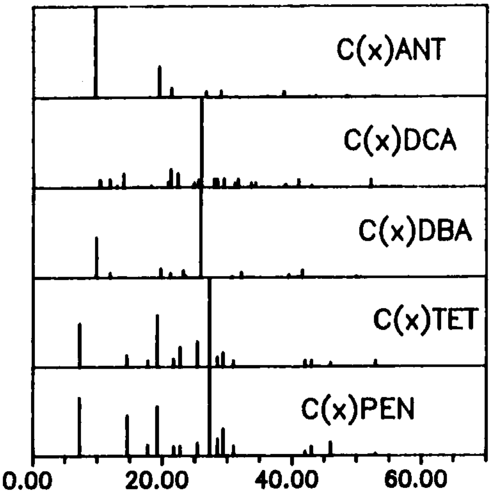

FIGURE 2. X-ray powder diffraction data for C_xPEN, $C_{78}TET$, $C_{37}DBA$, $C_{38}DCA$, and $C_{23}ANT$.

Because the van der Waals thickness of an aromatic hydrocarbon is indistinguishable from that of a graphite layer, elemental analysis results were necessary for interpretation of the X-ray data. For example, the composition of the anthracene intercalate was found to be C_{24}·ANT. Calculations indicate that each ANT in a close-packed array of ANT oriented parallel to the host layers will "cover" approximately 13 C atoms of a graphite layer, suggesting a second stage intercalate (Figure 3). Similarly, the observed C_{74}·TET stoichiometry suggests the presence of 5 carbon layers per 2 TET molecules, since each TET covers 31 C atoms of graphite, leading to a predicted stoichiometry of $C_{77.5}$·TET for a mixed

2nd and 3rd stage compound. The similarity of the X-ray data for C_x·PEN and C_{74}·TET suggests similar structure for both. Two arrangements of the DXA molecules are consistent with the X-ray data: a triple layer of DXA's with their planes parallel to the host layers, and a single layer of DXA's with the X---X axis perpendicular to the host layers (Figure 3). The former predicts a stoichiometry of C_{33}·DXA, the latter C_{39}·DXA, in marginally better agreement with the observed value. The latter is also reminiscent of the structure of Br_2-intercalated graphite, in which the Br atoms nest inside hexagons of C atoms in the host layers.[5] More detailed structural studies are clearly necessary.

TABLE I. Physical Data for the Graphite Intercalates, C_x·(Guest)

Intercalant	a(Å)	b(Å)	c(Å)	Staging	VDW gap expansion	x (found)	x (calc)	color
PEN	4.96	4.25	24.45	2nd/3rd	3.17	-	-	blue-black
TET	4.96	4.25	24.23	2nd/3rd	3.19	74	78	gold
ANT	4.96	4.12	10.00	2nd	3.21	24	26	black-green
DBA	7.42	6.43	17.64	2nd	10.94	37	39	yellow
DCA	7.41	6.38	16.96	2nd	10.26	38	39	yellow

Resistivity measurements showed that all the intercalates except that with DBA exhibited increased resistivity vs. graphite, while the resistivity of the DBA intercalate was essentially identical to that of graphite. Sonication of pristine graphite had essentially no effect. All intercalates were diamagnetic, with gram susceptibilities of -1.1 to $-1.2x10^6$ emu/g.

Layered Halide Intercalates

The apparent absence of an intercalation chemistry for normal-valent metal halides with layered structures is puzzling, and has been noted earlier.[6] The problem has been simply that most halides are sufficiently reactive that the host layers dissolve and react under conditions where many other materials exhibit intercalation chemistry. Our solution has been to utilize solvents and guests that do not dissolve or induce chemical reactions. Under these conditions, intercalation reactions can be observed. Some of compounds prepared to date are summarized in Table II.

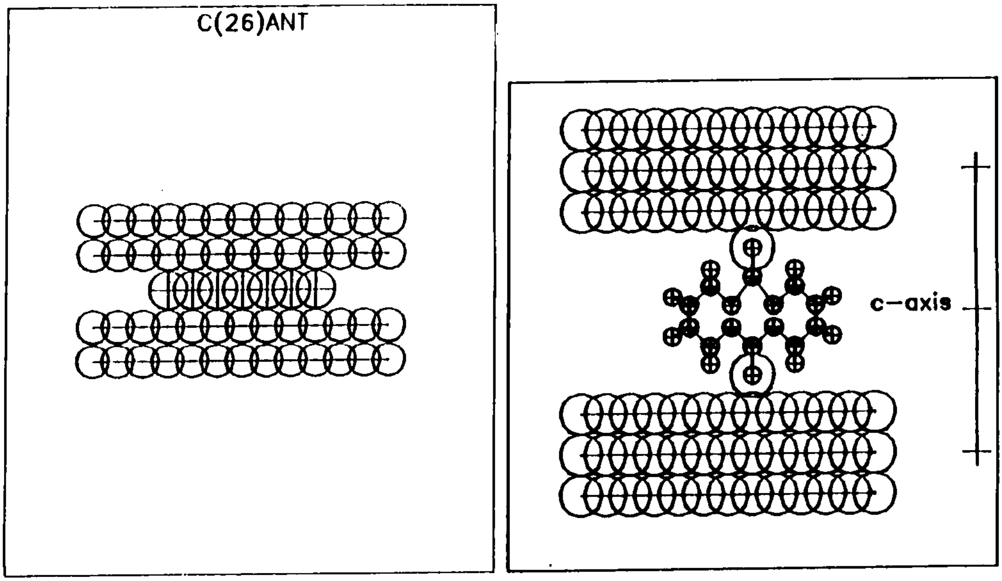

FIGURE 3. Schematic drawing of the proposed structure of C_{23}·ANT (left) and C_{39}·DXA (right). Open overlapping circles denote the carbon of the graphite layers: (left) the overlapping crossed circles denote the carbon atoms of ANT; (right) the small crossed circles denote the hydrogen and carbon of the DXA molecule, and the large circles with a crossed circle in the center denote the halogen.

TABLE II. Structural and Compositional Data for the MX_2 Intercalates MX_x·$(Guest)_y$

M	X	x	Guest	y	Color	Δc (Å)
Cu	Br	2.0	TET	0.84	orange-black	7.14
Cd	Br	2.0	TET	n.d.	gold	14.01
Cd	I	2.0	TET	n.d	gold	14.12
Ni	Br	1.73	TCN-TTF	0.33	purple	10.51
Cu	Cl	2.03	TCN-TTF	0.32	purple	9.50
Cu	Br	1.79	TCN-TTF	0.33	blue-black	10.84
Cd	Br	2.00	TCN-TTF	0.33	purple	10.06
Cd	I	2.05	TCN-TTF	0.74	black-violet	9.77

All compounds gave high quality X-ray powder diffraction data that could be indexed using an orthorhombic unit cell with $\underline{a} \sim 2\,\underline{a}^*$ and $\underline{b} \sim \sqrt{3}\,\underline{a}^*$ ($\underline{a}^*$ is the $\underline{a}$ parameter of the hexagonal host unit cell). The TET intercalates of CdI_2 and $CdBr_2$ appear to have the TET molecules oriented with their long axis essentially perpendicular to the host layers, since the layer expansion observed is essentially identical to the van der Waals length of TET (13.9 Å). In contrast, the $CuBr_2$ intercalate appears to have the TET molecules oriented with the molecular plane perpendicular to the host, but with the long axis parallel to the host layers, since the observed $\Delta\underline{c}$ is essentially the width of TET (7.2 Å). The TCN-TTF intercalates are more interesting, and appear to be oriented with the molecular plane perpendicular to the hosts but with the long axis tilted by ca. 50° from the horizontal, as shown in Figure 4. This structure allows two of the nitriles of each TCN-TTF to interact with metal ions in the host layers above and below in a Lewis base fashion. Since the van der Waals thickness of TCN-TTF is slightly greater than the X-X separation in all of the metal halides except CdI_2, only every other row of metal sites can be occupied. In the case of CdI_2, occupancy of all metal rows is possible, leading to a ca. 2-fold increase in guest to host ratio.

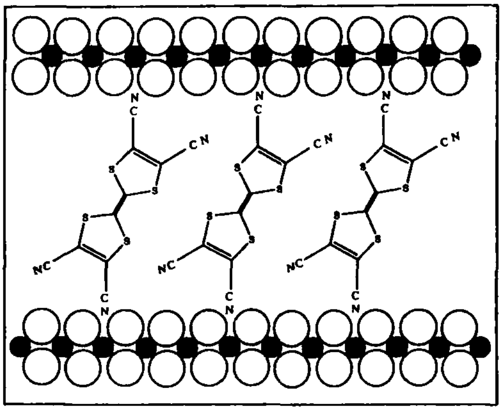

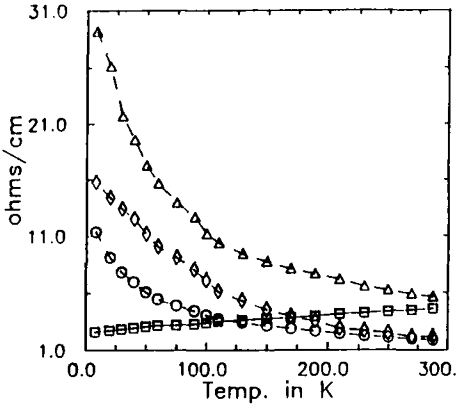

FIGURE 4 (left). Proposed arrangement of TCNTTF in MX_2 hosts. Large open circles denote the halide, and the small open circles denote the metal centers of the layers.

FIGURE 5 (right). Plots of resistivity vs. temperature for $(TCN\text{-}TTF)_{0.33}CuCl_{2.01}$ (◇), $TCN\text{-}TTF)_{0.74}CdI_{2.05}$ (△), $(TCN\text{-}TTF)_{0.33}CuBr_{1.79}$ (□), and $(TCN\text{-}TTF)_{0.33}NiBr_{1.73}$ (o).

Resistivity data for pressed pellets of selected metal halide-TCN-TTF intercalates are shown in Figure 5. As expected, most of the materials are semiconductors, but the $CuBr_2$ intercalate exhibits apparently metallic behavior. This difference is also noted in the magnetic susceptibility data (not shown), where the $CuBr_2$ intercalate exhibits an essentially temperature-independent paramagnetism over the range 4-300K. In contrast the $CuCl_2$ and $NiBr_2$ intercalates show Curie law magnetic behavior very similar to that of the pristine hosts. Whether the apparent loss of Br in $CuBr_{1.79}(TCN\text{-}TTF)_{0.33}$ is real and indicates partial reduction of the $Cu\text{-}Br_x$ layers, leading to the observed anomalous behavior, is not clear at this time. It should be noted, however that the analogous $NiBr_{1.73}(TCN\text{-}TTF)_{0.33}$ shows no unusual properties.

Metal Dichalcogenide Intercalates

Using the method outlined earlier, it has proven possible to prepare a wide range of new intercalation compounds of the metal dichalcogenides with aromatic guests. Some of the species prepared to date are shown in Table III, which also summarizes some of their properties.

TABLE III. Transition metal dichalcogenide intercalates of aromatic hydrocarbons and dibenzotetrathiafulvalene, $MY_2\cdot(Guest)_x$

Host	Guest	x	Δc(Å)	Color	Host	Guest	x	Δc(Å)	Color
TiS_2	ANT	0.17	3.39	black	$TiSe_2$	TET	0.50	17.65	gold
$TiSe_2$	ANT	0.24	3.25	black	TaS_2	TET	0.58	18.43	gold
TaS_2	ANT	0.18	3.34	black	$TaSe_2$	TET	0.59	16.75	gold
$TaSe_2$	ANT	0.18	3.47	black	$NbSe_2$	TET	0.63	16.16	gold
$NbSe_2$	ANT	0.19	3.39	black	$NbTe_2$	TET	0.66	17.02	gold
$NbTe_2$	ANT	0.22	3.38	black	TiS_2	PEN	0.44	22.85	black
TiS_2	DBTTF	0.54	19.56	orange	$TiSe_2$	PEN	1.85	34.32	black
$TiSe_2$	DBTTF	0.55	19.15	orange	TaS_2	PEN	0.66	23.78	blue-black
TaS_2	DBTTF	0.55	19.88	orange	$TaSe_2$	PEN	0.49	18.62	black
$TaSe_2$	DBTTF	0.67	20.05	orange	$NbSe_2$	PEN	0.39	22.18	black
TiS_2	TET	0.56	17.33	gold					

All of the materials showed well-defined X-ray powder patterns, which could be indexed using an orthorhombic unit cell as for the metal dihalide intercalates. For all the ANT intercalates, the observed interlayer expansion of ca. 3.4 Å and the stoichiometry indicate that the ANT is oriented parallel to the host layers. In contrast, the data for the TET, PEN (except $TiSe_2$•PEN), and DBTTF intercalates show much larger interlayer expansions and higher stoichiometries, which are most consistent with formation of a bilayer of guest species stacked with an interplanar distance of ca. 3.3 Å and tilted from the perpendicular by ca. 50°, as shown in Figure 6. The key point is that the observed values of $\Delta \underline{c}$ are <u>larger</u> than the length of TET (13.9 Å), PEN (16.1 Å), or DBTTF (15.3 Å), indicating that a single layer of guest molecules cannot account for the observed layer spacing. In the case of TiS_2•PEN, the interlayer distance is much larger ($\Delta \underline{c}$ = 34.3 Å), corresponding to approximately twice the length of the PEN molecule, and the observed stoichiometry is much higher (1.85 vs. 0.4-0.6). This suggests the presence of a perpendicular double layer of PEN molecules (Figure 7, for which a stoichiometry of $TiSe_2(PEN)_{1.95}$ is calculated.

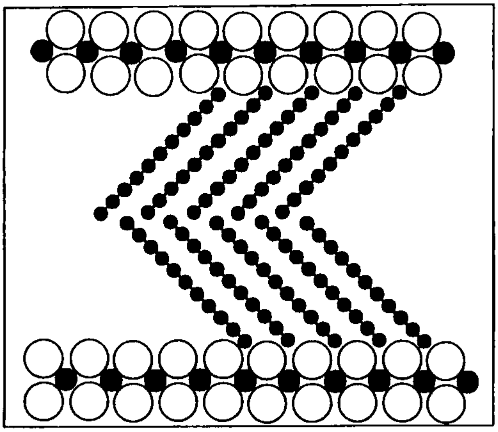

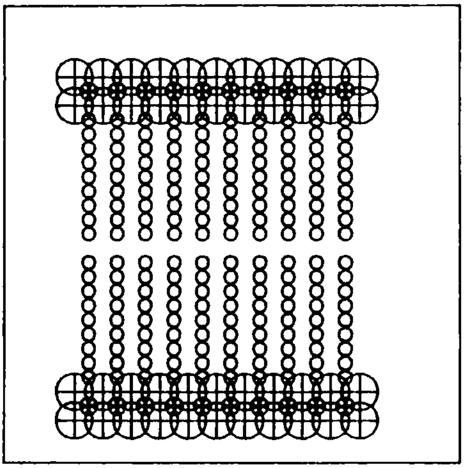

FIGURE 6 (left). Schematic drawing of the structure proposed for the $MY_2(TET)_x$ intercalates. A similar structure appears to be valid for the DBTTF and PEN intercalates except $TiSe_2(PEN)_{1.85}$.

FIGURE 7 (right). Schematic of the structure proposed for $TiSe_2(PEN)_{1.85}$.

Resistivity data measured on pressed pellets of the intercalates show that all of the TET and DBTTF intercalates and most of the ANT and PEN intercalates exhibit increases in resistivity ranging from small to rather large, with ANT typically giving the smallest increases. In contrast, $TaS_2(ANT)_{0.18}$, $TaS_2(PEN)_{0.66}$, and $TaSe_2(PEN)_{0.49}$ showed very small or no increase in resistivity vs. the pristine hosts. The $TaS_2(PEN)_{0.66}$ material showed a superconducting transition temperature of 7.05K, which is the highest T_c reported for any TaS_2 derivative.[7]

Fullerene Intercalates

The focus of previous research on the intercalation of fullerenes has been on their use as hosts capable of being intercalated by guests such as alkali metals.[8] The existence of the aromatic hydrocarbon intercalates discussed above prompted us to examine the potential of C_{60} to act as a guest capable of intercalation into layered hosts. We find that use of a double displacement technique, in which the host layers are first intercalated by a readily removable guest, acts to open up the layers for intercalation of C_{60}/C_{70} into TaS_2 and graphite. Experiments to date have been carried out with crude fullerenes, containing an 90:10 ratio of C_{60}:C_{70}. Properties of the resulting intercalates are summarized in Table IV. Schematic X-ray powder diffraction patterns are given in Figure 8. The $TaS_2(C_{60})_{0.174}$ data were indexed using an orthorhombic unit cell, and showed 00ℓ lines up to $\ell = 8$, while the graphite·C_{60} data shoved 00ℓ up to $\ell = 10$ and were readily indexed using a hexagonal unit cell. The compositions and structures are interpreted in terms of C_{60} as the guest, although the presence of significant amounts of C_{70} is possible. (Experiments with pure C_{60} are in progress.) The interlayer expansion of 10.26 Å observed for $TaS_2(C_{60})_{0.174}$ is consistent with formation of a first stage intercalate containing a single layer of C_{60} between the host layers. If the C_{60} units are close packed, a stoichiometry of $TaS_2(C_{60})_{0.175}$ is calculated, in excellent agreement with experiment. The observed c-axis of 17.2 Å for graphite·C_{60} is most consistent with a second-stage compound, containing two 3.35 Å thick graphite layers and one layer of C_{60}. A stoichiometry of $C_{60}·C_{56}$ is predicted if the C_{60} units form a commensurate 4x4 lattice due to the fortuitous close match between the diameter of C_{60} (ca. 10.2 Å) and the center-to-center repeat distance of the hexagons in graphite (2.46 Å). Determination of the stoichiometry of graphite·C_{60} is non-trivial, however. Proposed structures are shown in Figure 9.

TABLE IV. Properties of the Fullerene Intercalates of TaS_2 and Graphite, Formulated as Host$\cdot(C_{60})_x$

Host	x	a (Å)	b (Å)	c (Å)
TaS_2	0.174	6.792	5.910	16.11
graphite	n.d.	2.459 Å	-	17.21

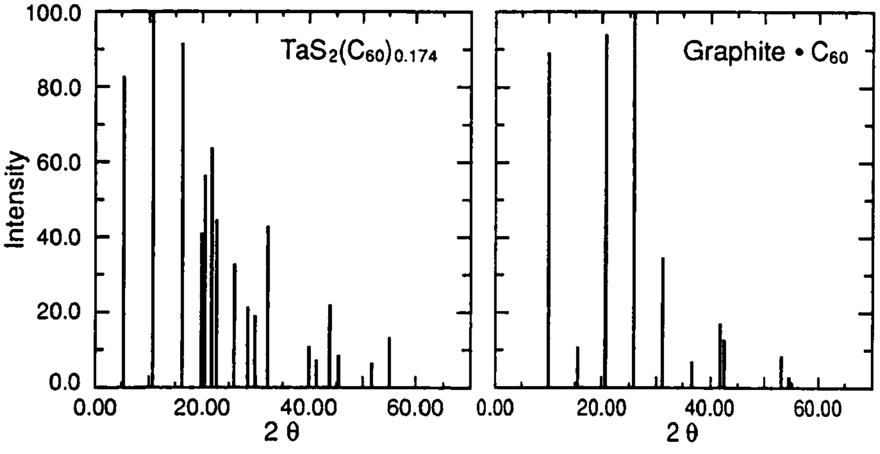

FIGURE 8. Schematic X-ray powder diffraction diagrams for $TaS_2(C_{60})_{0.174}$ (left) and graphite$\cdot C_{60}$ (right).

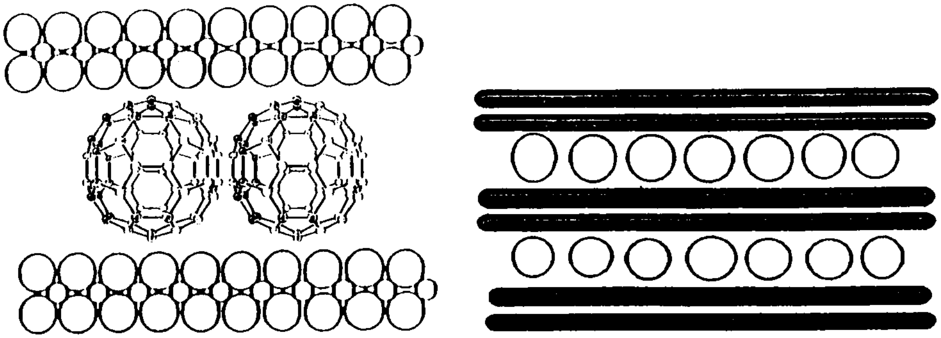

FIGURE 9. Proposed structures for $TaS_2(C_{60})_{0.174}$ (left) and graphite$\cdot C_{60}$ (right).

Resistivity measurements show that $TaS_2(C_{60})_{0.174}$ exhibits rough semiconducting behavior, with increased resistivity at lower temperatures, but a log plot of resistivity vs. 1/T is distinctly non-linear. This may be due to changes in the rotational mobility of the intercalated C_{60} as a function of temperature. Comparable data could not be obtained for graphite$\cdot C_{60}$, which could not be compacted under pressure. Instead, it acted as a fluid under pressure, escaping from the die. This suggests potential applications as, e.g., a lubricant.

CONCLUSIONS

(1) It has been possible to prepare bulk samples of layered metal dihalide intercalates for the first time, simply by avoiding solvents and reagents that promote net chemical reactions.

(2) Intercalation of simple aromatic hydrocarbons into a variety of layered hosts has been demonstrated. In most cases, it is difficult to envision a significant charge transfer between the guests and the hosts, suggesting that simple hydrophobic (van der Waals) forces are most important and that the intercalation of these guests can be viewed as a process of dissolution in the host. The colors observed for some of the materials may be due to the presence of intense π-π^* transitions in the guests rather than to plasma edges.

(3) Fullerenes (C_{60}/C_{70}) have been used as guests and shown to intercalate into TaS_2 and graphite.

ACKNOWLEDGEMENTS

This research was supported by the U.S. Office of Naval Research (N0014-91-J-1962 to B.A.A.) and in part by NATO (0727-87 to B.A.A. and J.-M.F.). We thank Ben Brandt for assistance with the figures.

REFERENCES

1. M. S. Whittingham and A. J. Jacobson, Intercalation Chemistry (Academic Press, New York, 1982).
2. M. J. McKelvy and W. S. Glaunsinger, Ann. Rev. Phys. Chem., 41, 497 (1990).
3. R. Schöllhorn, H. D. Zagefka, T. Butz, and A. Lerf, Mater. Res. Bull., 14, 369 (1979).
4. C. W. Clark, D. K. Smith, and G. Johnson, Fortran IV X-Ray Powder Diffraction Program (1973).
5. S. M. Heald and E. A. Stern, Phys. Rev. B, 17, 4069 (1978).
6. J. D. Corbett, in Ref. 1, p. 361.
7. A. H. Thompson and F. J. DiSalvo, in Ref. 1, p. 584.
8. J. E. Fischer, P. A. Heiney, D. E. Luzzi, and D. E. Cox, in Fullerenes, edited by G. S. Hammond and V. J. Kuck (ACS Symp. Ser. 481, 1992) Ch. 4, pp. 55-69.